九州大学学術情報リポジトリ
Kyushu University Institutional Repository

Performance Characteristics of a Deformed 120-Degree Partial Bearing with Couple Stress Lubrication

Sanjeev Kumar Lambha
Department of Mechanical Engineering National Institute of Technology

Kumar, Vinod
Department of Mechanical Engineering National Institute of Technology

Verma, Rajiv
Department of Mechanical Engineering National Institute of Technology

https://doi.org/10.5109/4793662

出版情報：Evergreen. 9 (2), pp.269-282, 2022-06. 九州大学グリーンテクノロジー研究教育センター
バージョン：
権利関係：Creative Commons Attribution-NonCommercial 4.0 International

KYUSHU UNIVERSITY

Performance Characteristics of a Deformed 120-Degree Partial Bearing with Couple Stress Lubrication

Sanjeev Kumar Lambha*, Vinod Kumar, Rajiv Verma
Department of Mechanical Engineering
National Institute of Technology, Kurukshetra
Kurukshetra, Haryana, India

*Author to whom correspondence should be addressed:
E-mail: sanjeev.lambha@gmail.com

(Received February 8, 2022; Revised May 18, 2022; accepted June 4, 2022).

Abstract: The influence of using a fluid with couple stresses as lubricant on the performance of 120° partial bearing is studied here. The effect of variation in liner deformation is also considered. Modified Reynold's equation along with the elasticity equation is solved by using an FEM approach to predict the properties in static and dynamic form. The properties studied are peak pressure, carrying capacity of load, stiffness characteristic, damping characteristics. Based on the results it is concluded that for a deformed bearing liner dynamic performance of 120° partial bearing are enhanced by using the fluid with couple stresses.

Keywords: Couple stress fluid, liner deformation, partial arc bearing, elastohydrodynamic lubrication, static characteristics, dynamic characteristics.

1. Introduction

The classically used lubrication phenomenon is hydrodynamic which plays a major role in the operation of rotating machines. For smooth functioning of interrelated parts of any machine, the journal bearing is a key element used from past decades for transmission of power and to withstand loads between mating parts. The properties of Newtonian lubricant, used classically can be improved by adding some chemical compounds (additives) in the base fluid. The addition of these long chain polymer additives into the Newtonian fluids makes them to be non-Newtonian. One such kind of non-Newtonian lubricant is a fluid with couple stresses popularly known as couple stress fluid. The rheological behaviour in fluid with couple stresses is based on the theory of micro continuum[1)] The effect of fluid with couple stresses was studied by many researchers to predict its effects on the performance of journal bearings. The load capacity was improvised, and friction coefficient reduced on addition of polymer particles to lubricants[2-3)]. An action of squeezing in bearing with partial arc[4)] was presented by authors for fluid with couple stresses. The load capacity of cylindrical bearing operating with liner deformation and couple stresses were enhanced[5)]. The key factors: bearing geometric features, factor of couple stress and magnetic based parameters governs the load capacity and film thickness[6)]. The wear and friction near edges decreased by using couple stresses in finite line contacts[7)]. A 3-D elasticity model was used for couple stresses and elasticity parameter to evaluate the static, dynamic and stability characteristics of cylindrical bearing[8)]. The rheological effects of a fluid with couple stresses improved the dynamic performance[9)] of hydrodynamic bearings. The influence of textured surfaces observed to be more significant compared to non-textured surfaces for a fluid with couple stresses[10)]. The load carrying capacity, attitude angle, friction coefficient, side leakage of journal bearing was improved for a combined effect of the turbulence and elasticity of bearing liner[11)]. The new material constant η is completely responsible for the couple stress property of fluid. The effect of variation in viscosity of fluid on bearing performance was studied by many researchers from a long decade. A combined influence[12)] of viscosity variation, velocity slip and couple stresses studied for pressure and the load capacity. A review study of micropolar fluids, power-law fluids and couple stress lubricants resulted that the non-Newtonian lubricants gives better results compared to Newtonian[13)]. The selection of right lubricant with appropriate couple stress properties resulted an enhancement in the stability range and damping abilities[14)] for two lobe non-circular journal bearings. A lubrication model considering the effect of misalignment, couple stress and shear thinning impacts the sensitivity of fluid lubrication in proportion to couple stress parameter, such that for an area of minimum film thickness, the sensitivity is maximum[15)].

The film thickness in clearance space depends on type of bearing used. Depending on the type of applications, bearings are classified from geometry point of view, according to which bearing are of two types broadly, full arc (360° arc length) bearings which encircles the shaft completely and partial arc (less than 360° arc length) bearings. The number of partial arcs are connected with each other to form the category of lobed bearings. Most common type of partial bearings is a 180° arc bearing, but the bearing with an arc length of 120° are used in several cases. Partial arc bearings are used for the applications of relatively low-speeds and load in constant direction, but due to their significant role in lobed bearings it is required to study their behaviour. A study to predict the behaviour of bearing with partial arc as static and dynamic characteristics[16] agreed with the data available by Raimodi. The authors proposed an inexpensive, fast and accurate approach[17] for the solution of Reynold's equation. In an experimental study of a 60° bearing for two clearance ratios and the Reynolds number up to 12000 a good resemblance[18] founded for some particular range of empirical factor whereas beyond this range the correlation becomes poorer. The performance of 120° partial bearing showed that for maximum load capacity and lowest friction the clearance ratio and pivot location were closest to optimum for varying compressibility factor[19]. A design chart[20] for centrally loaded partial bearing was presented for gas lubrication. The increase in factor of misalignment and non-Newtonian lubricant decreased the load in a partial bearing[21]. The impact of lubrication with couple stresses on the performance of a skeletal joint[22] application was studied.

The deformation of bearing liner creates an expansion in clearance space and consecutively the thickness of fluid also gets expanded. This change in the fluid film thickness due to deformation of bearing liner effects the performance of the journal bearing. For an accurate and perfect design of partial bearing it is important to consider the elasticity of the liner during analysis. The influence of deformation in bearing liner on 60° and 120° centrally loaded bearings[23] showed that the effect of deformation coefficient on a bearing arc of short span (60°) is more compared to a long span (120°). The influence of resilience in liner was studied[24] to know the performance of cylindrical bearing. An approach with the combination of FEM and boundary element was used[25] to predict the impact of deformation in housing. The impact of flexibility in bearing liner for determination of deformation coefficient parameter was defined relatively by the factors[26] R_j, C, t, μ, U_o and E_m. The dimensions of bearings and their stiffness was studied for an application of connecting rod housing[27]. A deterministic numerical solution[28] was used to know the combined impact of pad deformation and mixed lubrication on performance of partial bearing. The effect of static and dynamic deformation on the performance characteristics and stability parameters of a journal bearing was studied for water lubrication and rubber liner[29]. A closed form approximate solution was used to solve the modified Reynold's equation for partial bearing with lubrication of couple stresses[30]. A combined effect of deformed liner and couple stresses recorded that the systems operating with a fluid of couple stresses have better dynamic response compared to Newtonian fluid[31]. The lubricant types and their viscosities investigated to know their effects on compressor and system performance[32] for the development of new lubricants to use in heat pump. The particles effect for spiral and circular pipes investigated the non-Newtonian fluid rheology[33]. Finite Element Analysis was used to model the knee prosthesis to know static and cyclic loads[34]. A comparative study[35] of friction coefficient between Aluminium Alloy 5083 block and SKD 11 disk resulted that the use of RBD palm oil minimizes friction in a lower manner than the use of SAE40 engine oil. The nonedible nanofluids was analysed[36] to study its tribological performance through four ball test, which summarized MJOa2 a suitable fluid for fluid applications of metal working. A study of review[37] for additives of Nanoparticles and their mechanisms highlighted the tribological effects of NP's in lubrication to reduce wear and friction. The combined influence of fluid with couple stresses and pressure-viscosity variation on the parallel plates of triangular shape[41] analysed to study their squeeze performance. It was founded that the introduction of couple stresses in fluid with variation of viscosity improved the performance characteristics in comparison to Newtonian iso-viscous lubricant. The use of Jakobson-Floberg Ollson (JFO) condition of cavitation effects the tribological performance for a known value of load prominently by using couple stress fluid[42] which presented a significant effect on performance for texture shape but slight for texture distribution. The exact solution of pressure gradient, pressure rise, velocity and stream function were obtained for a peristaltic transport pattern of couple stress fluid[43] to know the impact of lateral walls and partial slip. The use of couple stress fluid in an analysis of three-lobe journal bearing[44] improved their dynamic stability whereas an increase in critical mass and decrease in whirl frequency was observed for an improvement of stability range. The consideration of radiation and viscous dissipation effect in biconvective MHD flow analysis for couple stress fluid showed an increase in thermal boundary layer for Brinkman number and a reverse trend for concentration boundary layer[45]. On analysing the performance of journal bearing for couple stress fluid, misalignment, surface roughness and thermal effect, an enhancement in all performance characteristics was observed except side leakage for an increase in couple stress parameter[46].

Based on literature, it is observed that the influence of couple stresses on the performance of a partial bearing with the consideration of liner deformation is not reported till date. This paper presents the study of a 120° partial

bearing lubricated with a fluid of couple stresses for elasto-hydrodynamic lubrication. The properties of the bearing in terms of static and dynamic are evaluated and presented. For an effective and fast solution of the system equations numerically, an approach of FEM (i.e. *Finite Element Method*) is used for analysis. This analysis helps the designers to design the partial bearing of this kind for the fulfilment of increasing demands to provide a better life to bearing systems.

2. Analysis

The influence of using a lubrication of couple stresses in 120° partial arc bearings are analyzed here in this study. The effect of flexibility in liner is also considered to know its impact on the performance of bearing. The geometrical representation of partial bearing is shown in Fig. 1, where the journal is characterized by center O_j and radius R_j whereas the bearing is characterized by center O_b and radius R_b. The body forces and body couples are assumed to be absent in the lubricating fluid blended with long chain polymer additives. The characteristics of fluid with couple stresses are characterized by a factor (l), which depends on new material constant denoted by η. The modified Reynold's equation with fluid of couple stresses for partial bearing is solved along with an elasticity equation for liner deformation to calculate the characteristics of journal bearing statically and dynamically.

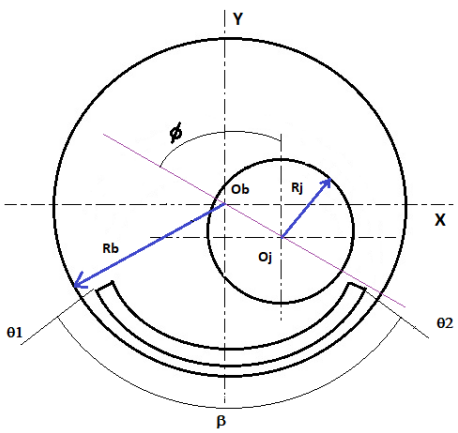

Fig. 1: Geometric representation of bearing with partial arc

The set of equations used for the modelling of the system are explained below.

2.1. The modified Reynold's equation

The action of fluid flow with couple stresses in between the surfaces of journal and bearing liner is expressed by a fluid flow equation. The continuity equation and momentum equation used to find the fluid flow equation based on the stokes model[1)] are expressed as:

$$\rho \frac{Dv}{Dt} = -\nabla p + \rho \boldsymbol{F} + {}^{1}/_{2}\, \rho \nabla * \boldsymbol{C} + \mu \nabla^2 - \eta \nabla^4 \boldsymbol{V} \quad (1)$$

$$\nabla \boldsymbol{V} = 0 \quad (2)$$

where, $\boldsymbol{V}$ *= Velocity vector,*

$\boldsymbol{F}$ *= Body force for unit mass,*

$\boldsymbol{C}$ *= Body couple for unit mass,*

ρ *= Density,*

μ *= shear viscosity,*

p *= pressure,*

η *= material constant defines the couple stress property of fluid.*

The motion equation in Cartesian coordinate with assumptions can be expressed as:

$$\frac{\partial p}{\partial x} = \mu \frac{\partial^2 u}{\partial y^2} - \eta \frac{\partial^4 u}{\partial y^4} \quad (3)$$

$$\frac{\partial p}{\partial y} = 0 \quad (4)$$

$$\frac{\partial p}{\partial z} = \mu \frac{\partial^2 w}{\partial y^2} - \eta \frac{\partial^4 w}{\partial y^4} \quad (5)$$

$$\frac{\partial u}{\partial x} + \frac{\partial v}{\partial y} + \frac{\partial w}{\partial z} = 0 \quad (6)$$

u, v, w denotes the velocity components in x, y, z directions.

The boundary conditions applicable to bearing as well as journal surfaces are:

$$u_{y=0} = 0;\ v_{y=0} = 0;\ w_{y=0} = 0 \quad (7.1)$$

$$\frac{\partial^2 u}{\partial y^2}_{y=0} = \frac{\partial^2 w}{\partial y^2}_{y=0} = 0 \quad (7.2)$$

$$u_{y=h} = U;\ v_{y=h} = V;\ w_{y=h} = 0 \quad (8.1)$$

$$\frac{\partial^2 u}{\partial y^2}_{y=h} = \frac{\partial^2 w}{\partial y^2}_{y=h} = 0 \quad (8.2)$$

The velocity components after integrating equation (3) and equation (5) by considering boundary conditions are as follows:

$$u = U\, {}^{y}/_{h} + {}^{1}/_{2\mu} \frac{\partial p}{\partial x} \left\{ y(y-h) + 2l^2 \left(1 - \frac{\cos h\left(\frac{2y-h}{2l}\right)}{\cos h\left({}^{h}/_{2l}\right)} \right) \right\} \quad (9.1)$$

$$w = \frac{1}{2\mu} \frac{\partial p}{\partial z} \left\{ y(y-h) + 2l^2 \left(1 - \frac{\cos h\left(\frac{2y-h}{2l}\right)}{\cos h\left({}^{h}/_{2l}\right)} \right) \right\} \quad (9.2)$$

where, $l = \sqrt{{}^{\eta}/_{\mu}}$, characteristic length.

The non-dimensional form of modified Reynold's equation for fluid flow in present case is expressed as,

$$\frac{\partial}{\partial\theta}\left(\frac{G(\bar{h},l^*)}{\bar{\mu}}\frac{\partial\bar{p}}{\partial\theta}\right)+\frac{1}{4\lambda^2}\frac{\partial}{\partial\bar{Z}}\left(\frac{G(\bar{h},l^*)}{\bar{\mu}}\frac{\partial\bar{p}}{\partial\bar{Z}}\right)=6\frac{\partial\bar{h}}{\partial\theta}+12\frac{\partial\bar{h}}{\partial\tau} \quad (10)$$

where, $G(\bar{h},l^*)=\bar{h}^3-12l^{*2}\bar{h}+24l^{*3}\tan h\left(\frac{\bar{h}}{2l^*}\right)$

The factors for non-dimensionalisation of the system are considered and mentioned as:

$\theta=\frac{X}{R_j}$; $\bar{Z}=\frac{Z}{L}$; $\lambda=\frac{L}{2R_j}$; $\bar{h}=\frac{h}{c}$; $h=1+\varepsilon\cos\theta$; $\varepsilon=\frac{e}{c}$; $\bar{p}=\frac{pc^2}{\mu_0\omega_j R_j^2}$; $\bar{\mu}=\frac{\mu}{\mu_0}$; $\tau=\omega_j t$; $U=R_j\omega_j$; $l^*=\frac{l}{c}$; $l=\left(\frac{\eta}{\mu}\right)^{1/2}$

It is experienced practically that the pressure developed into the fluid film creates an impact on the surface of the liner at an interface of fluid film and bearing liner. As it is assumed that the material used for bearing liner is more elastic than journal, so the liner gets displaced, and changed the thickness of fluid film which is expressed as:

$$\bar{h}=1-(\bar{X}j-\Delta\bar{X})\cos\theta-(\bar{Z}j-\Delta\bar{Z})\sin\theta+\bar{\delta}r \quad (11)$$

such that $\bar{X}j=\varepsilon\sin\phi$, & $\bar{Z}j=-\varepsilon\cos\phi$,

where, $\bar{X}j$ & $\bar{Z}j$ = the steady state coordinates of journal center, $\Delta\bar{X}$ & $\Delta\bar{Z}$ = perturbation components of journal center from steady state, $\bar{\delta}r$ = the radial deformation of bearing liner.

2.2. FEM formulation of Reynolds equation

A mathematical approach of *Finite Element Method* is used to solve the set of equations. So the FEM formulation of fluid flow equation is expressed in this section. An elemental four noded bilinear isoparametric model is adopted for discretization of fluid film, such that the film is discretized as a node size of 50X40 in tangential and axial direction. The pressure $\bar{p}$ for each noded element is expressed as:

$$\bar{p}^e=\sum_{i=1}^{i=4}N_i\,\bar{p}_i^e \quad ; \quad (12)$$

where, N_i = shape function for the ith node, & $\bar{p}_i^e$= corresponding nodal pressure of eth element

The Galerkin's orthogonal residual approach is used to solve the Reynold's equation in FEM formulation, and the equation is expressed as:

$$\sum_{i=1}^{i=n}\iint\left[\frac{\partial}{\partial\theta}\left(\frac{G(\bar{h},l^*)}{\mu}\frac{\partial p^e}{\partial\theta}\right)+\frac{\partial 1}{4\lambda^2}\frac{\partial}{\partial\bar{Z}}\left(\frac{G(\bar{h},l^*)}{\mu}\frac{\partial p^e}{\partial\bar{Z}}\right)-6\frac{\partial\bar{h}}{\partial\theta}-12\frac{\partial\bar{h}}{\partial\tau}\right]N_i^e\,d\theta\,d\bar{Z}=0 \quad (13)$$

It can also be written as

$$\sum_{i=1}^{i=n}\left([F_{ij}^e][\bar{p}_i^e]-[A_{ij}^e]-[B_i^e]\right)=0 \quad (14),$$

From equation (14);

$$[F_{ij}^e]=\iint_{A^e}\left\{G(\bar{h},l^*)\left[\frac{\partial N_i^e}{\partial\theta}\frac{\partial N_j^e}{\partial\theta}+\frac{\partial N_i^e}{\partial\bar{Z}}\frac{\partial N_j^e}{\partial\bar{Z}}\right]\right\}d\theta d\bar{Z} \quad ,$$

(15.1) i, j = 1,2,3,4

$$[A_{ij}^e]=6\iint_{A^e}\bar{h}\frac{\partial N_i^e}{\partial\theta}d\theta d\bar{Z}, \quad (15.2)$$

i, j = 1,2,3,4

$$[B_i^e]=12\iint_{A^e}\bar{h}\frac{\partial N_i^e}{\partial\tau}d\theta d\bar{Z}=0 \text{ (for static analysis)}$$

(15.3) i, j = 1,2,3,4

The expression for complete domain of fluid flow is expressed as:

$$[F_{ij}][\bar{p}_i]=[A_{ij}] \quad (16)$$

where, $[F_{ij}]$ = Assembled coefficient matrix also known as *fluidity matrix*, $[A_{ij}]$ = Assembled column vector consisting of vector terms, $[\bar{p}_i]$ = Nodal pressure vector.

The pressure distribution for a flexible bearing is obtained by solving equation (10) along with an elasticity equation. The expression used to know the impact of deformation in bearing liner is discussed in section below.

2.3. The deformation in liner of Bearing

The flexibility of the liner compared to the journal and bearing housing effects the liner to be deformed under the action of pressure induced at film liner interface. The deformation of bearing liner is considered while design for practical functioning of bearings. The liner is discretized as an isoparametric, 8-noded hexahedral elemental model as shown in Fig. 2. At each node the liner displacement is in three directions viz. circumferential, radial & axial as δ_x, δ_y & δ_z. For calculation of deformation in liner due to film thickness, only radial (δ_y) component is considered as the effect of tangential force is negligible for the present analysis.

The displacement in three direction is represented by, $\delta=\begin{Bmatrix}\delta x\\ \delta y\\ \delta z\end{Bmatrix}$, and for this study the expression used for deformation is $\delta_r=\begin{Bmatrix}0\\ \delta y\\ 0\end{Bmatrix}$ as only radial deformation is considered here.

The deformation of liner in radial direction is obtained by using an elasticity equation[8)] for the discretized bearing liner which is expressed as:

$$[\bar{K}]\{\bar{\delta}_r\}=C_d\{\bar{F}\} \quad (17)$$

where, $[\bar{K}]=\left(1/_{E_L R_j}\right)[K]$ *(stiffness matrix)*

(18.1) $\left(\because [K]^e=\int_V\bar{B}^T\bar{D}\bar{B}dV^e\right)$

$\{\bar{F}\}=\left(c^2/_{\bar{p}\mu_0\omega_j R_j^4}\right)\{F\}$*(surface traction vector)*

$$(18.2)\quad \left(\because \{F\}^e = \int_{A^e} N^T F dA^e\right)$$

$$\{\bar{\delta}_r\} = \left(\frac{1}{c}\right)\{\delta_r\} \text{ (displacement vector)}$$

$$(18.3)\quad \left(\because \{\delta_r\} = (C_d \times \bar{p})\right)$$

$$C_d = \left(\frac{\mu_0 \omega_j}{E}\right)\left(\frac{t\bar{h}}{R_j}\right)\left(\frac{R_j^3}{c^3}\right) \text{(coefficient of deformation)} \quad (18.4)$$

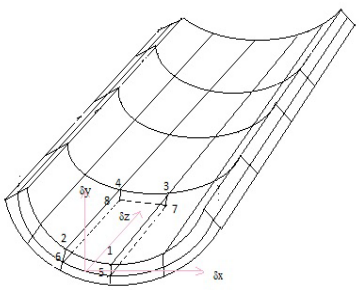

Fig. 2: Eight-noded hexahedral discretised bearing liner

2.4. Performance Characteristics

The pressure obtained from an iterative solution of modified Reynold's equation along with elasticity equation is used to calculate the various characteristics of bearing with partial arc. The behavior of the system is predicted and represented by plotting the variation of static characteristics and dynamic characteristics with the change of eccentricity ratio. The performance characteristics of the system calculated statically are explained below:

Load Bearing Capacity:

The capacity of bearing load in a partial bearing can be calculated by using the expressions[26] of radial and tangential components as:

$$\bar{W}_x = \int_{\theta_1}^{\theta_2}\int_{-1}^{+1} \bar{p}\cos\theta \, d\theta d\bar{z}, \&$$

$$\bar{W}_z = \int_{\theta_1}^{\theta_2}\int_{-1}^{+1} \bar{p}\sin\theta \, d\theta d\bar{z} \quad (19)$$

The net load and attitude angle of the bearing is obtained by using the expression below:

$$\bar{W} = \sqrt{\bar{W}_x^2 + \bar{W}_z^2};\ \tan\emptyset = \frac{\bar{W}_z}{\bar{W}_x} \quad (20)$$

The Somerfield number can be expressed as:

$$S = \frac{2\lambda}{\pi\bar{W}} \quad (21)$$

The dynamic properties give a measure to the time-dependent behaviour of the system. The dynamic response for the system of journal bearing is calculated by obtaining the associated stiffness and damping characteristics, which are expressed as:

$$\begin{bmatrix}\bar{K}_{xx} & \bar{K}_{xz}\\ \bar{K}_{zx} & \bar{K}_{zz}\end{bmatrix} = -\int_{\theta_1}^{\theta_2}\int_{-1}^{+1}\begin{bmatrix}\frac{d\bar{p}}{d\bar{X}}\\ \frac{d\bar{p}}{d\bar{Z}}\end{bmatrix}[\cos\theta \quad \sin\theta]d\theta d\bar{Z}$$

(22.1)

$$\begin{bmatrix}\bar{C}_{xx} & \bar{C}_{xz}\\ \bar{C}_{zx} & \bar{C}_{zz}\end{bmatrix} = -\int_{\theta_1}^{\theta_2}\int_{-1}^{+1}\begin{bmatrix}\frac{d\bar{p}}{d\dot{\bar{X}}}\\ \frac{d\bar{p}}{d\dot{\bar{Z}}}\end{bmatrix}[\cos\theta \quad \sin\theta]d\theta d\bar{Z}$$

(22.2)

$\frac{d\bar{p}}{d\bar{X}}, \frac{d\bar{p}}{d\bar{Z}}, \frac{d\bar{p}}{d\dot{\bar{X}}}, \frac{d\bar{p}}{d\dot{\bar{Z}}}$ are obtained by solving the Reynolds's equation expressed above.

The non-dimensional form of linearized motion equation is:

$$[\bar{M}_j]\left[\ddot{\bar{X}}\right] = [\bar{C}_{ij}]\left[\dot{\bar{X}}\right] + [\bar{K}_{ij}][\bar{X}]; \quad [\bar{M}_j]\left[\ddot{\bar{Z}}\right] = [\bar{C}_{ij}]\left[\dot{\bar{Z}}\right] + [\bar{K}_{ij}][\bar{Z}] \quad (23)$$

Thus, equation for distributed motion of journal can be expressed as:

$$[\bar{M}_j]\begin{bmatrix}\ddot{\bar{X}}\\ \ddot{\bar{Z}}\end{bmatrix} = \begin{Bmatrix}\Delta F_X(\bar{X},\bar{Z},\dot{\bar{X}},\dot{\bar{Z}})\\ \Delta F_Z(\bar{X},\bar{Z},\dot{\bar{X}},\dot{\bar{Z}})\end{Bmatrix} \quad (24),$$

$$[\bar{M}_j] = \begin{bmatrix}\bar{M}_j & 0\\ 0 & \bar{M}_j\end{bmatrix} = \text{(diagonal mass matrix)},$$

$\begin{bmatrix}\ddot{\bar{X}}\\ \ddot{\bar{Z}}\end{bmatrix}$ = the components of acceleration in X & Z directions, ΔF_X & ΔF_Z = unbalance forces on journal in X & Z directions.

After substituting the respective values, an equation of motion can be expressed as:

$$\bar{M}_j\ddot{X} - \bar{C}_{XX}\dot{\bar{X}} - \bar{C}_{XZ}\dot{\bar{Z}} - \bar{K}_{XX}\bar{X} - \bar{K}_{XZ}\bar{Z} = 0\ ;\ \bar{M}_j\ddot{Z} - \bar{C}_{ZX}\dot{\bar{X}} - \bar{C}_{ZZ}\dot{\bar{Z}} - \bar{K}_{XZ}\bar{X} - \bar{K}_{ZZ}\bar{Z} = 0 \quad (25)$$

The characteristic equation in polynomial form can be written as:

$$\sigma^4 + A_1\sigma^3 + A_2\sigma^2 + A_3\sigma + A_4 = 0 \quad (26)$$

Where, σ = Complex variable, A_i = function for mass coefficients. i = 1, 2, 3…….

The stability characteristics i.e. critical mass *(M_c)*, threshold speed (ω_{th}), whirl frequency (*υ*) is obtained by solving polynomial form of characteristic equation using Routh's criteria. Threshold speed (the speed of journal at instability threshold) is calculated by the use of expression as expressed below:

$$\omega_{th} = \sqrt{\frac{\bar{M}_c}{\bar{W}}} \quad (27)$$

where, $\bar{M}_c = KI/\nu^2$

$$\nu^2 = \frac{(\bar{K}_{XX}-KI)(\bar{K}_{ZZ}-KI)-\bar{K}_{XZ}\bar{K}_{ZX}}{(\bar{C}_{XX}\bar{C}_{ZZ}-\bar{C}_{XZ}\bar{C}_{ZX})}, \quad (28)$$

(*υ* is the whirl frequency ratio at threshold instability)

$$KI = \frac{(\bar{K}_{XX}\bar{C}_{ZZ}+\bar{K}_{ZZ}\bar{C}_{XX}-\bar{K}_{XZ}\bar{C}_{ZX}-\bar{K}_{ZX}\bar{C}_{XZ})}{(\bar{C}_{XX}+\bar{C}_{ZZ})} \quad (29)$$

2.5. Solution Procedure

The set of equations used in present study are solved by applying an iterative scheme/procedure to find the

nodal pressure in first stage. The system initialized by storing some initial values of ε and ϕ along with the other required geometric properties into the memory of program. The elastic deformation of liner changes the film thickness under various loading conditions for bearing with partial arc, due to which the pressure at different node positions also changes. The nodal pressures at various nodes are used to find the performance characteristics further in second stage of solution procedure.

The boundary conditions for the system are stated as:

$\bar{p} = 0 \; at \; \bar{z} = -1$; $\bar{p} = 0 \; at \; \bar{z} = +1$; $\bar{p} = 0 \; at \; \bar{z} = \beta_1$; $\bar{p} = 0 \; at \; \bar{z} = \beta_2$; $\left(\frac{\partial \bar{p}}{\partial \alpha}\right)_{\alpha_2} = 0$; $\left(\frac{P_i^k - P_{i-1}^k}{P_i^k}\right) < (1/10^5)$, *Criteria for pressure convergence,*

(27) *i is iteration index and k = 1,2, 3…. n.*

The sketch of solution procedure is shown in Fig. 3.

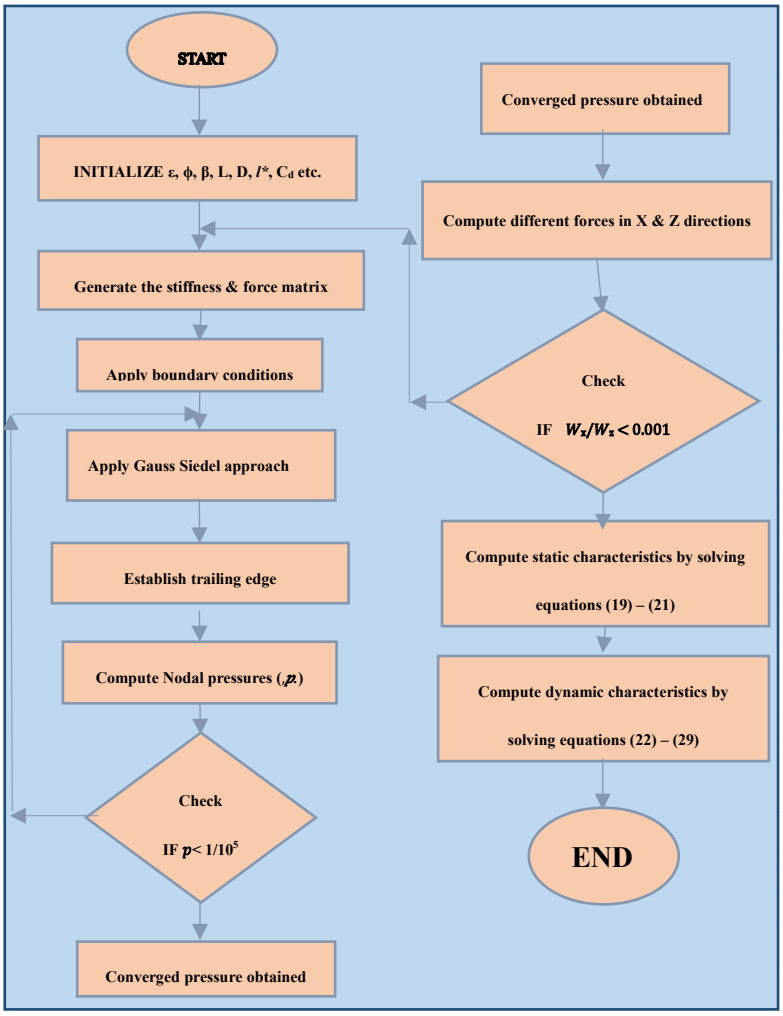

Fig. 3: Solution Procedure

3. Results and Discussions

The lubrication in the performance of a journal bearing is of great importance, as the properties of lubricant used have an influence on the thickness of fluid film which is a key factor responsible for the hydrodynamic action in system using journal bearing with partial arc. In an elasto-hydrodynamic lubrication analysis, the material for liner is softer than the material used for journal and bearing housing. Therefore, due to difference in pressure at the interaction of surfaces, a deformation in liner is produced. The behavior of journal bearing with partial arc in terms of static and dynamic properties for an arc length (β) 120°, couple stress parameter (l^*) as 0.0 (rigid), 0.05, and 0.15, and the deformation coefficient (C_d) as 0.0, 0.3 and 0.5 is studied here. To check the affirmation of model and solution procedure used, the results are validated with the published results. The validation of attitude angle in relation to load carrying[38] and eccentricity ratio[40] is presented in Fig. 4. The program used is validated by comparing the results of 120° partial arc bearing in Table 1. For dynamic characteristics, a circular bearing is validated for stiffness and damping characteristics[8] as shown in Fig. 5.

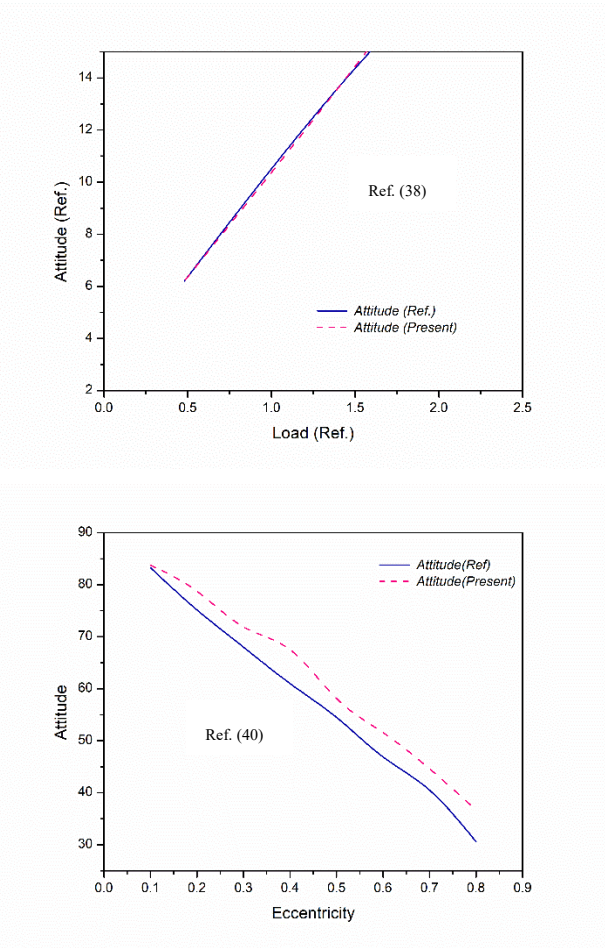

Fig. 4: Validation of attitude angle

Table 1. Validation of results with published results for β = 120°, C_d=0.0 and λ = 1.0

Validation	Validation of Load characteristics (β = 120°, C_d=0.0 and λ = 1.0)						
	ε= 0.1	ε = 0.2	ε = 0.3	ε = 0.4	ε = 0.5	ε = 0.6	ε = 0.7
Load by Ref. (23)	0.36	0.64	1.05	1.75	2.5	3.95	6.3
Load by Present	0.29459 8678	0.6349 21731	1.0570 34318	1.6461 69757	2.5269 19162	3.9308 78482	6.46199 5914
% deviation	-18.056	-0.781	0.667	-5.943	1.080	-0.481	2.571
Validation	Validation of Pressure characteristics (β = 120°, C_d=0.0 and λ = 1.0)						
	ε = 0.1	ε = 0.2	ε = 0.3	ε = 0.4	ε = 0.5	ε = 0.6	
Pressure by Ref. (23)	0.2	0.4	0.65	1.105	1.7	2.755	
Pressure by Present	0.17215 5961	0.3768 23593	0.6445 08865	1.0393 98577	1.6672 51688	2.7600 56022	
% deviation	-13.922	-5.794	-0.845	-5.937	-1.926	0.184	

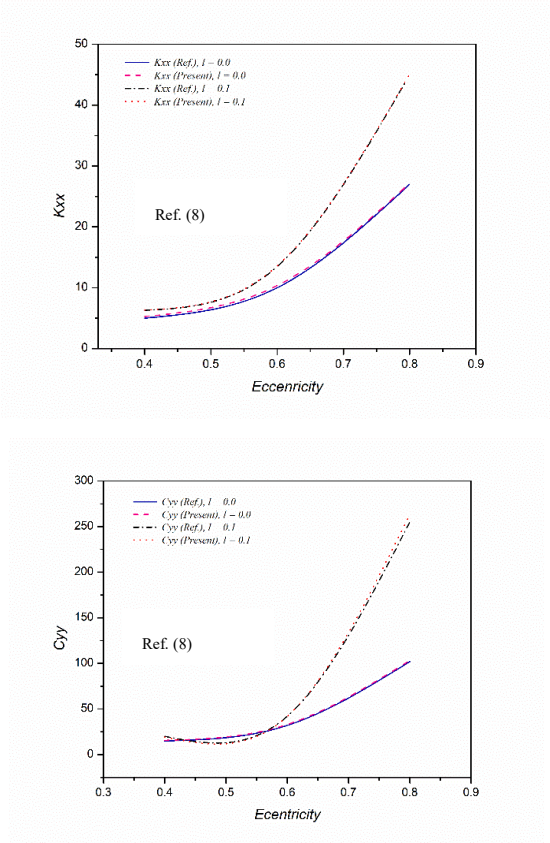

Fig. 5: Validation of dynamic characteristics

On comparing, the results calculated using present program, with available results of reference, it shows a good agreement. The only difference shown here is due to the difference in approach used.

3.1. Static Properties

The properties which are statically associated with the system and varying very slowly or remains constant with time are termed as the static characteristics. It is observed and depicted from the contours of pressure plot with circumferential positions, that how a pressure is varying for the partial bearing operating with a fluid of couple stresses. From Fig. 4 (a) – (f) it is clearly obvious that for hydrodynamic lubrication (C_d = 0.0), the peak pressure is increased by using the fluid with couple stresses compared to a Newtonian fluid. On increasing the value of couple stress parameter (*CSP*) (l^* = *0.0 – 0.15)* there is an improvement in the value of peak pressure. For a deformed liner (C_d = 0.5) i.e. elasto-hydrodynamic lubrication also, the peak pressure is improved on increasing the (*CSP*) (l^* = *0.0 – 0.15).* On the other hand, it is observed by comparing the contours of deformed (C_d = 0.5) and undeformed (C_d = 0.0) partial bearings that the pressure is reduced for a deformed bearing in comparison to an undeformed/ rigid bearing.

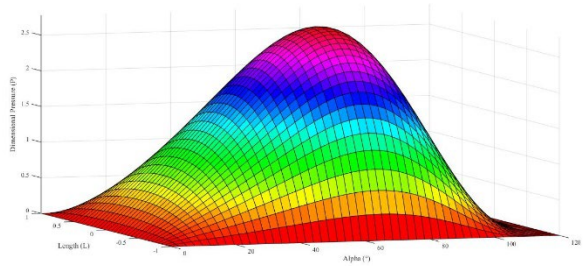

a. Pressure field in hydrodynamic partial bearing with Newtonian Fluid (l = 0.0)*

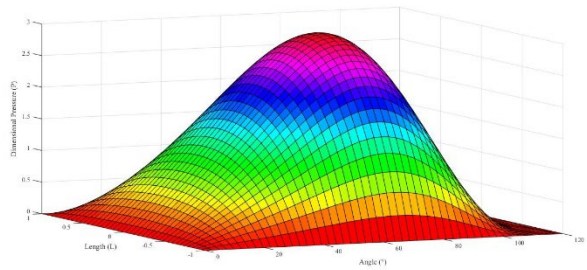

b. Pressure field in hydrodynamic partial bearing with (CSF) (l = 0.05)*

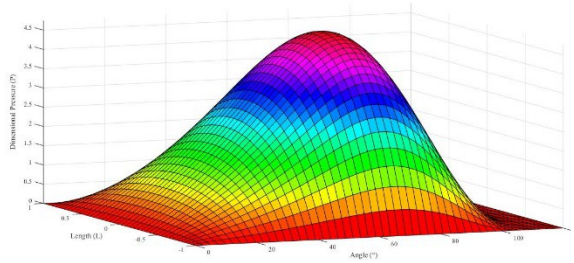

c. Pressure field in hydrodynamic partial bearing with (CSF) (l = 0.15)*

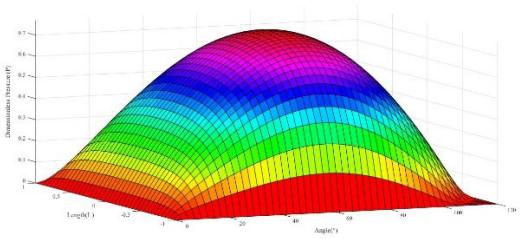

d. Pressure field in elasto-hydrodynamic partial bearing with Newtonian Fluid (l = 0.0)*

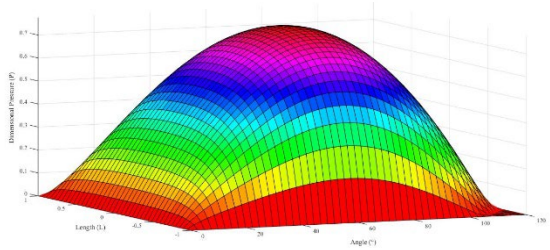

e. Pressure field in elasto-hydrodynamic partial bearing with (CSF) (l = 0.05)*

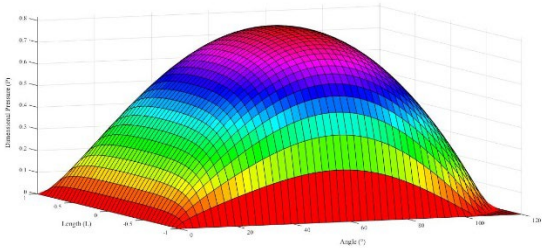

f. Pressure field in elasto-hydrodynamic partial bearing with (CSF) (l = 0.15)*

Fig. 6: Pressure distributed in discretized domain of partial journal bearing for ε = 0.6 and λ = 1.0
(a) C_d = 0.0, l* = 0.0 (b) C_d = 0.0, l* = 0.05
(c) C_d = 0.0, l* = 0.15 (d) C_d = 0.5, l* = 0.0
(e) C_d = 0.5 l* = 0.05 (f) C_d = 0.5, l* = 0.15

The variation of pressure along the circumferential direction is also clearly predicted by observing and analyzing the plots of contours for fluid film thickness in discretized domain as shown in Fig. 7 and plots of pressure at center line shown by Fig. 8. By analyzing Fig. 7 & Fig. 8, it is observed that on comparing the length of fluid film thickness for C_d = 0.0 & 0.5, the trailing edge for the deformed bearing is found to appear up to a large circumferential angle compared to rigid bearings. It is also observed from the plots generated in Fig. 7 & Fig. 8, that at any particular value of C_d the peak pressure is increased with an increase in the value of (*CSP*).

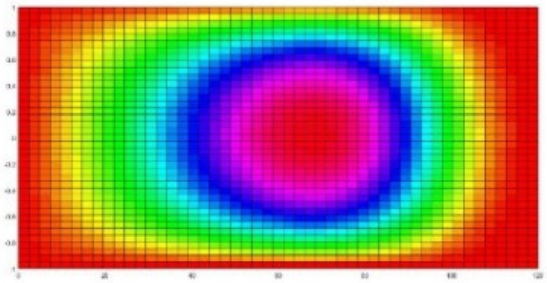

(a)

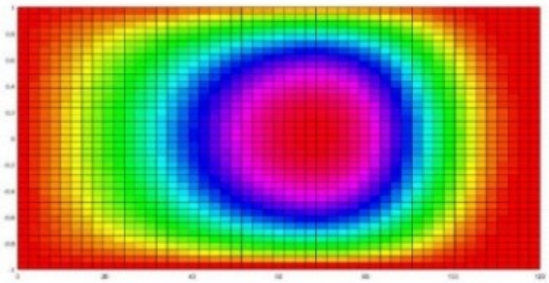

(b)

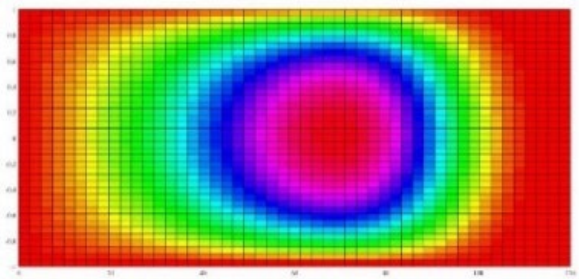

(c)

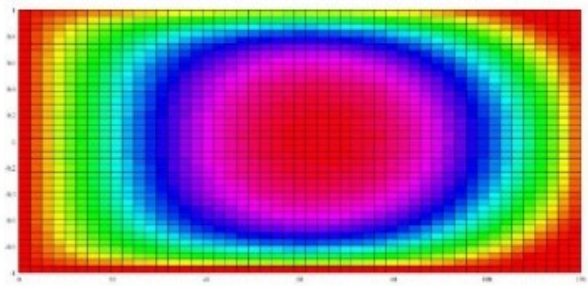

(d)

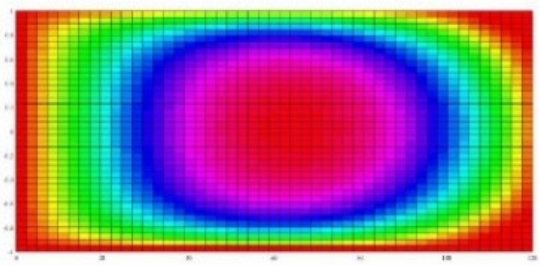

(e)

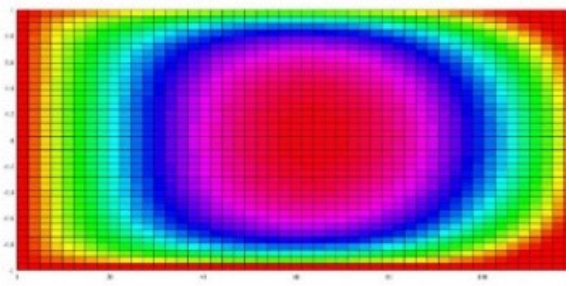

(f)

Fig. 7: Fluid film thickness in discretized domain of partial journal bearing for ε = 0.6 and λ = 1.0
(a) C_d = 0.0, l* = 0.0 (b) C_d = 0.0, l* = 0.05
(c) C_d = 0.0, l* = 0.15 (d) C_d = 0.5, l* = 0.0
(e) C_d = 0.5 l* = 0.05 (f) C_d = 0.5, l* = 0.15

This increase in peak pressure shows that the load carrying increases with increasing the couple stress property in fluids.

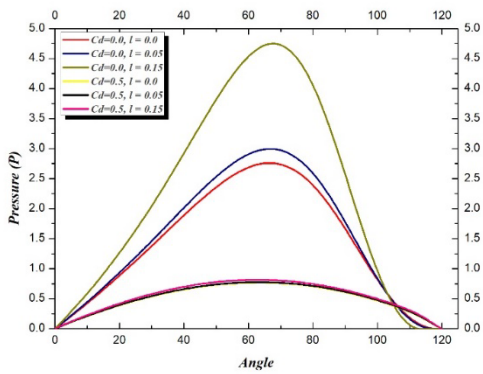

Fig. 8: Pressure at the centre line (P) with Circumferential angle

For more understanding of changes in carrying capacity of loads for the system of bearing under analysis, the plot of Load (*W*) with eccentricity ratio is presented in Fig. 9. It is obvious from Fig. 9 that the load carrying is increased on moving from Newtonian to a fluid with couple stresses. The carrying capacity of load is also increases with an increase in (*CSP*) i.e. l^* = 0.0 – 0.15 for all values of eccentricity ratios. The change in deformation of bearing liner creates an impact on the load carrying in such a way that for a bearing with deformed liner the carrying capacity of load is lesser than the load for a bearing with rigid liner. The load is also effecting by enhancing the eccentricity ratio such that the carrying load for higher eccentricity ($\varepsilon = 0.8$) is higher than the carrying load for lower eccentricity ($\varepsilon = 0.1$).

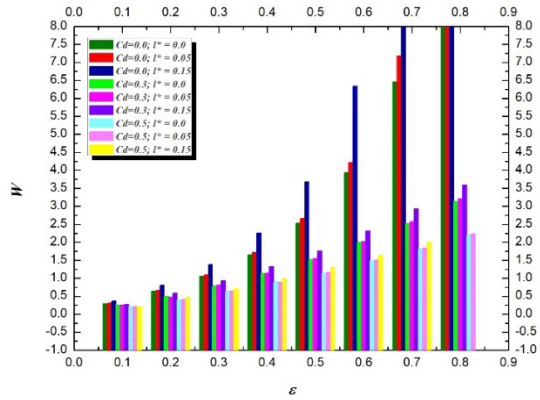

Fig. 9: Load bearing capacity ($\overline{W}$) with Eccentricity (ε)

The influence of using a fluid with couple stresses and change in liner deformation on the static characteristics are discussed in this section. Likewise, the static properties the characteristics responded dynamically are also influenced due to change in fluid property and variation in the thickness of bearing liner. The characteristics which shows changes in dynamic behavior of a bearing with partial arc are presented in form of stiffness and damping properties in the plots presented in Fig. 10-13 in the section below.

3.2. Stiffness and Damping characteristics

The influence of change in fluid property on the stiffness and damping characteristics of a partial bearing system are presented in Fig. 10-13.

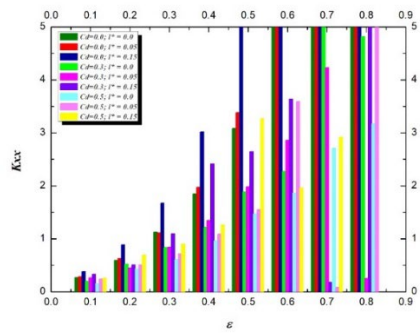

(a)

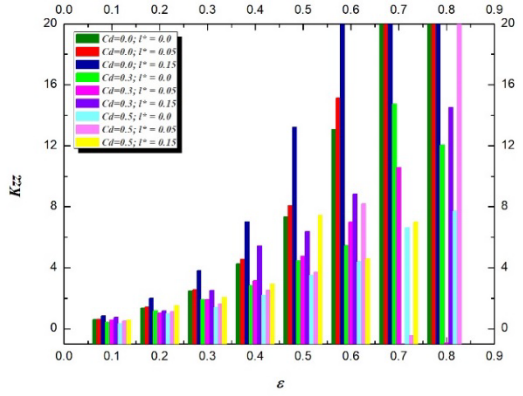

(b)

Fig. 10: Direct Coupled Stiffness ($\bar{K}_{xx}$, $\bar{K}_{zz}$) with Eccentricity (ε): (a) $\bar{K}_{xx}$, (b) $\bar{K}_{zz}$

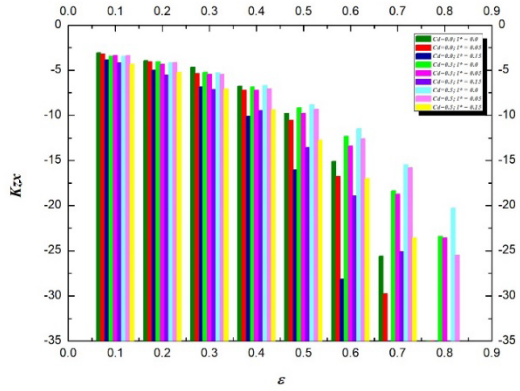

(b)

Fig. 11: Cross-Coupled Stiffness ($\bar{K}_{xz}$, $\bar{K}_{zx}$) with Eccentricity (ε): (a) $\bar{K}_{xz}$, (b) $\bar{K}_{zx}$

Fig. 10 shows the variation of direct stiffness properties along the eccentricity ratio ranges from $\varepsilon = 0.1$ to $\varepsilon = 0.8$. The direct stiffness $\bar{K}_{xx}$ & $\bar{K}_{zz}$ are increasing for the value of (*CSP*) moving as $l^* = 0.0 – 0.05 – 0.15$, for both the rigid as well as deformed liner. Whereas, The value of $\bar{K}_{xx}$ & $\bar{K}_{zz}$ is deceased with an increase in coefficient of deformation (C_d) for all the values of (*CSP*).

Fig. 11 (a)-(b) represents the variation of crossed stiffness with eccentricity ratios, The plot for crossed stiffness indicates that there is an increase in $\bar{K}_{xz}$ for an increasing value of (*CSP*) as $l^* = 0.0 – 0.05 – 0.15$, whereas $\bar{K}_{zx}$ shows a trend of decrement for an increase in parameter of couple stresses. The plots states that for an increase in the coefficient of deformation (C_d), the $\bar{K}_{xz}$ shows an increment, whereas the $\bar{K}_{zx}$ shows a decrease in its form. It is also observed from Fig. 11 (b) that the values of $\bar{K}_{zx}$ are negative for all the values of (*CSP*) and deformation coefficients as well. The negative values of crossed stiffness indicate that the system is exhibiting a destabilizing manner and it is needed to stabilize the system which requires the higher number of perturbations for this purpose.

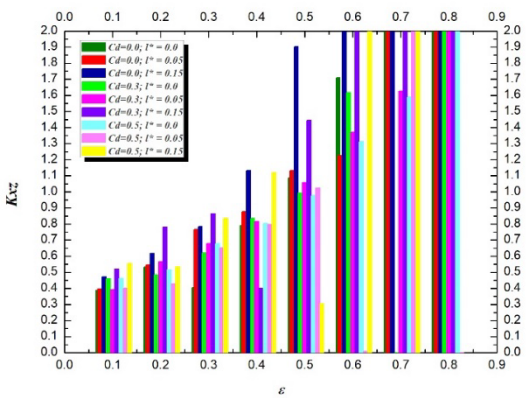

(a)

The damping coefficients are the key parameters which explain the stabilization of the system in nonlinear motion due to disturbances with time. The influence on the damping characteristics in bearing of partial arc operating with a fluid of couple stresses are presented in Fig. 12-13. It is shown in Fig. 12 (a)-(b) that how the direct damping coefficients varies with an increase in (*CSP*) (l^*) and parameter for deformation of bearing liner *(C_d)*. The coefficient of direct damping coefficient $\bar{C}_{xx}$ and $\bar{C}_{zz}$ both are increased with an increase in the value of (*CSP*) as $l^* = 0.0 – 0.05 – 0.15$. The direct damping $\bar{C}_{xx}$ and $\bar{C}_{zz}$ both are increasing slowly with an increase in (C_d) for small values of eccentricity ratios i.e. $\varepsilon = 0.1 – 0.2$, but for higher eccentricity ratios i.e. $\varepsilon = 0.3$ onwards the plots for direct damping coefficients shows a trend of decrement in in its form with an increase in (C_d). Fig. 13 gives us the results for variation of crossed damping coefficients with l^* and *(C_d)* along the range of eccentricity ratios $\varepsilon = 0.1 – 0.8$. The value of crossed damping is decreased with an increase in (*CSP*) up to an eccentricity ratio $\varepsilon = 0.6$.

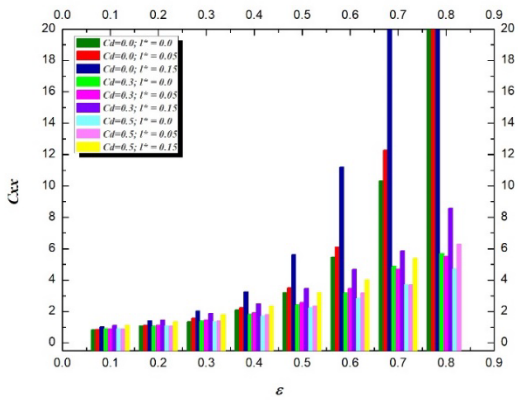

(a)

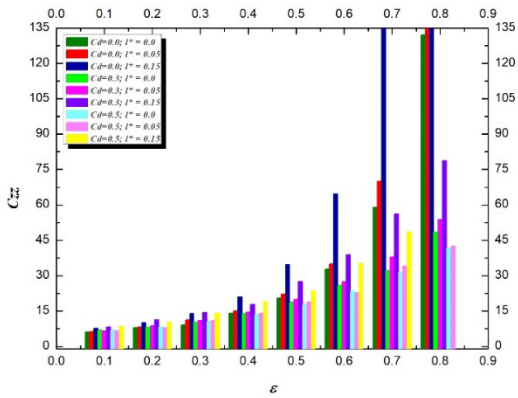

(b)

Fig. 12: Direct Coupled Damping ($\bar{C}_{xx}$, $\bar{C}_{zz}$) with Eccentricity (ε): (a) $\bar{C}_{xx}$, (b) $\bar{C}_{zz}$

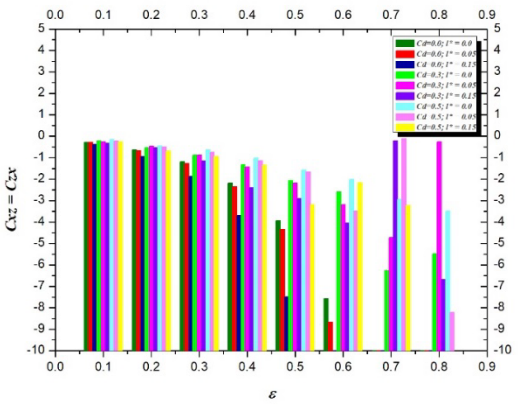

Fig. 13: Cross Coupled Damping ($\bar{C}_{xz} = \bar{C}_{zx}$) with Eccentricity (ε)

4. Conclusion

The influence of using a fluid with couple stresses and deformation in liner on the performance of a 120° arc partial bearing is studied here. The pressure developed in fluid film creates an impact on the liner and due to the elastic property of liner material the liner gets deformed which results an increase in the fluid film thickness. Its effects on associated static characteristics resulted an increase in peak pressures as well as load bearing capacity of both the rigid and deformed bearings by increasing the parameter of fluid with couple stresses *(l^*)*. The trailing edge is extended up to a greater circumferential angle in deformed bearings compared to rigid bearings.

The dynamic performance is shown by stiffness and damping characteristics according to which the direct stiffness $\bar{K}_{xx}$ & $\bar{K}_{zz}$ for increasing (*CSP*) as l^* = 0.0 – 0.05 – 0.15 are increased for both the rigid as well as the deformed bearings, whereas, decreased with an increase in coefficient of deformation (C_d) for all the values of (*CSP*). The value of crossed damping is decreased with an increase in (*CSP*) up to an eccentricity ratio, ε = 0.6, but an increasing-decreasing trend for higher eccentricities shows that system is highly in destabilizing condition.

Thus, it is concluded that a 120° partial bearing operating with a fluid of couple stresses shows better performance compared to a bearing operating with Newtonian fluid. It is helpful for a designer to consider this study for designing of a partial bearing to use in an application of relatively low speed when load is acting in one direction.

Acknowledgements

I am highly thankful to my co-authors Prof. Vinod Kumar and Dr. Rajiv Verma for helping me to achieve the results of this research. I am thankful to the Head, Mechanical Engineering, NIT Kurukshetra for providing me the Lab facilities for getting the results.

Nomenclature

c	Radial clearance (mm), $c = R-r$
C_d	Deformation coefficient
C_{ij}	Damping coefficient (dimensional) (Ns/mm)
$\bar{C}_{ij}$	Damping coefficient (non-dimensional), $\bar{C}_{ij} = \frac{C_{ij}c^3}{\mu_0 R_j^4}$
$\bar{C}_{xx}, \bar{C}_{zz}$	Direct damping coefficients (non-dimensional)
$\bar{C}_{xz}, \bar{C}_{zx}$	Cross damping coefficients (non-dimensional)
D	Journal Diameter (mm), $D = 2R_j$
e	Eccentricity of journal (mm)
$[F]$	Surface traction vector
h	Fluid film thickness (dimensional) (mm)
$\bar{h}$	Fluid film thickness (non-dimensional), $\bar{h} = h/c$
K_{ij}	Stiffness coefficients (dimensional) (N/mm)
$\bar{K}_{ij}$	Stiffness coefficient (non-dimensional), $K_{ij} = \frac{K_{ij}c^3}{\mu_0 \omega_j R_j^4}$
$\bar{K}_{xx}, \bar{K}_{zz}$	Direct stiffness coefficients (non-dimensional)
$\bar{K}_{xz}, \bar{K}_{zx}$	Cross stiffness coefficients (non-dimensional)
L	Length of bearing (mm)
l	Characteristic length of additives (mm), $l = (\eta/\mu)^{1/2}$
l^*	Dimensionless couple-stress parameter, $l^* = l/c$

$\bar{M}j$	Mass of journal (Kg)
$\bar{M}_c$	Critical mass of journal (Kg)
O_b	Centre of bearing
O_j	Centre of journal
p	Pressure distribution (dimensional) (N/mm^2)
$\bar{p}$	Pressure distribution (non-dimensional), $\bar{p} = \frac{pc^2}{\mu_0 \omega_j R_j^2}$
R_j	Radius of journal (mm)
S	Somerfield Number
t	Time (s)
W	Load bearing capacity (dimensional) (N)
$\bar{W}$	Load bearing capacity (non-dimensional), $\frac{Wc^3}{\mu_0 \omega_j R_j^4}$
$\bar{W}_x, \bar{W}_z$	Load in x direction and z direction
X_j, Z_j	Journal center coordinates
$\bar{z}$	Axial coordinate, $\bar{z} = Z/_{L}$
θ	Circumferential coordinate, θ = X/R
μ	Lubricant dynamic viscosity (Pa-s)
μ_0	Dynamic viscosity for reference (Pa-s)
$\bar{\mu}$	Dynamic viscosity (non-dimensional), $\bar{\mu} = \mu/_{\mu_0} = 1$
ω_j	Rotational speed of journal (rad/s)
ω_{th}	Threshold speed (non-dimensional)
Φ	Attitude angle (^{0})
η	new material constant peculiar to *CSF*
ε	Eccentricity ratio, $\varepsilon = e/c$
λ	Aspect ratio, $\lambda = L/D$
β	Arc length of partial arc bearing
β_1	Angular position at start of partial bearing
β_2	Angular position at end of partial bearing
δ_r	Radial deformation of bearing liner

References

1) V. K. Stokes "Couple Stresses in Fluids", *Springer, Berlin, Heidelberg*, (1966). doi: 10.1007/978-3-642-82351-0_4.
2) D. R. Oliver "Load enhancement effects due to polymer thickening in a short model journal bearing", *J. Nonnewton. Fluid Mech.*, 30(2–3), 185–196 (1988). doi: 10.1016/0377-0257%2888%2985024-9.
3) H. A. Spikes "The behaviour of lubricants in contacts: current understanding and future possibilities", *Part J: Journal of Engineering Tribology*, 208, 3-15 (2016). doi: 10.1243%2FPIME_PROC_1994_208_345_02.
4) J. R. Lin "Squeeze film characteristics of long partial journal bearings lubricated with couple stress fluids", *Tribology International*, 30(1), 53-58 (1997). doi: 10.5560/ZNA.2011-0009.
5) S. K. Lambha, V. Kumar, and R. Verma "Elastohydrodynamic analysis of couple stress lubricated cylindrical journal bearing", *Journal of Physics: Conference Series*, 1240(1) (2019). doi: 10.1088/1742-6596/1240/1/012165.
6) N. C. Das "A study of optimum load- bearing capacity for slider bearings lubricated with couple stress fluids in magnetic field", *Tribology International*, 31(7), 393–400 (1998). doi: 10.1016/S0301-679X(98)00050-4.
7) S. P. Chippa & M. Sarangi "Elastohydrodynamically lubricated finite line contact with couple stress fluids", *Tribology International*, 67, 11–20 (2013). doi: 10.1016%2Fj.triboint.2013.06.014.
8) P. K. Rohilla, R. Verma, and S. Verma "Performance analysis of couple stress fluid operated elastic hydrodynamic journal bearing", *Tribology Online*, 14(3), 143–154 (2019). doi: 10.2474/trol.14.143.
9) S. K. Guha "A theoretical analysis of dynamic characteristics of hydrodynamic journal bearings lubricated with coupled stress fluids", *Part J: Journal of Engineering Triboloy*, 125–133 (2015). doi: 10.1177%2F135065010421800207.
10) C. B. Khatri, and S. C. Sharma "Influence of couple stress lubricant on the performance of textured two-lobe slot-entry hybrid journal bearing system", *Journal of Engineering Tribology*, 1–19 (2016). doi: 10.1177%2F1350650116658377.
11) B. Chetti "Combined effects of turbulence and elastic deformation on the performance of a journal bearing lubricated with a couple stress fluid Governing equation", *Journal of Engineering Tribology*, 1–7 (2018). doi: 10.1177%2F1350650118757555.
12) T. Dass, S. Rao, and D. M. G. Comissiong "The combined effect of couple stresses , variable viscosity and velocity-slip on the lubrication of finite journal bearings", *Ain Shams Eng. J.*, 11(2), 501–518 (2020). doi: 10.1016/j.asej.2020.01.002.
13) R. K. Dang, D. Goyal, A. Chauhan, and S. S. Dhami "Effect of non-newtonian lubricants on static and dynamic characteristics of journal bearings", *Mater. Today Proceedings*, 23(3), 1345-1349 (2020). doi: 10.1016/j.matpr.2020.04.727.
14) M. Z. Mehrjardi "Dynamic stability analysis of noncircular two-lobe journal bearings with couple stress lubricant regime", *Proc. IMechE Part J: Journal of Engineering Tribology*, 235(6), 1150-1167 (2021). doi: 10.1177%2F1350650120945517.
15) J. Zhu "Analysis of misaligned journal bearing lubrication performance considering the effect of lubricant couple stress and shear thinning", *Journal of Mechanics*, 282–290 (2021). doi: 10.1093/jom/ufaa018.

16) P. C. Warner "Static and Dynamic Properties of Partial Journal Bearings", *Journal of Basic Engineering*, 247-255 (1963). doi: 10.1115/1.3656569.
17) R. J. Wernick, and C. H. T. Pan "Static and Dynamic Characteristics of Self-Acting, Partial-Arc, Gas Journal Bearings", *Journal of Basic Engineering*, 405-413 (1964). doi: 10.1115/1.3653089.
18) F. K. Orcutt "Investigation of a Partial Arc Pad Bearing in the Superlatninar Flow Regime", *Journal of Basic Engineering*, 145-152 (1965). doi: 10.1115/1.3650491.
19) E. J. Guntur Jr. "The Influence of Lubricant compressibility on the performance of the 120 degree partial journal bearing", *Journal of Lubrication Technology*, 473-481 (1967). doi: 10.1115/1.3617035.
20) M. Chandra, M. Malik, and R. Sinhasan "Gas bearings part II: Design data for centrally loaded partial arc journal bearings", *Wear*, 89(2), 163–171 (1983). doi: 10.1016/0043-1648/2883/2990241-7.
21) R. H. Buckholz, and J. F. Lin "The Effect of Journal Bearing Misalignment on Load and Cavitation for Non-Newtonian Lubricants", *Journal of Tribology,* 108, 645-654 (1986). doi: 10.1115/1.3261295.
22) T. V. V. L. N. Rao, A. Majdi, A. Rani, and G. Manivasagam "Squeeze Film Analysis of Three-layered Parallel Plate and Partial Journal Bearing Lubricated with Couple Stress Fluids for Skeletal Joint Applications", *Mater. Today Proc.*, 15, 328–335 (2019). doi: 10.1016/j.matpr.2019.05.013.
23) S. C. Jain, R. Sinhasan, and D. V. Singh "Elasto-hydrodynamic lubrication analysis of partial arc journal bearings" *Tribology International,* 161-168 (1982). doi: 10.1016/0301-679X(82)90135-9.
24) M. A. Hili, S. Bouaziz, M. Maatar, T. Fakhfakh, and M. Haddar. "Hydrodynamic and elastohydrodynamic studies of a cylindrical journal bearing" *J. Hydrodyn.*, 22(2), 155–163 (2010). doi: 10.1016/S1001-6058(09)60041-X.
25) K. Kohno, S. Takahashi, and K. Saki "Elasto-hydrodynamic lubrication analysis of journal bearings with combined use of boundary elements and finite elements", *Engineering Analysis with Boundary Elements,* 13, 273-281 (1994). doi: 10.1016/0955-7997(94)90053-1.
26) S. C. Jain, R. Sinhasan, and D. V. Singh "Elastohydrodynamic analysis of a cylindrical journal bearing with a flexible bearing shell", *Wear*, 78, 325–335 (1982).
27) Y. Okamoto, M. Hanahashi, and T. Katagiri "Effects of Housing Stiffness and Bearing Dimension on Engine Bearing Performance by Elastohydrodynamic Lubrication Analysis", *Journal of Tribology*, 122, 697-704 (2000). doi: 10.1115/1.1314604
28) M. B. Dobrica, M. Fillon, and P. Maspeyrot "Influence of mixed-lubrication and rough elastic-plastic contact on the performance of small fluid film bearings", *Tribology Transaction*, 51(6), 699–717 (2008). doi: 10.1080/10402000801888903.
29) M. Lahmar, S. Ellagoune, and B. Bou-saïd "Elastohydrodynamic Lubrication Analysis of a Compliant Journal Bearing Considering Static and Dynamic Deformations of the Bearing Liner", *Tribology Transaction,* 53, 349–368 (2010). doi: 10.1080/10402000903312356.
30) A. Ruggiero, A. Senatore, and S. Ciortan "Partial Journal Bearings With Couple Stress Fluids : An Approximate Closed-Form Solution", *Mechanical Testing and Diagnosis,* 2, 21-26 (2012).
31) B. Chetti, and W. A. Crosby "EHD Effect on the Dynamic Characteristics of a Journal Bearing Lubricated with Couple Stress Fluids", *Int. J. of Civil and Environmental Engineering,* 4(9), 1103–1108 (2016). doi: 10.5281/zenodo.1126145.
32) Y. Changru, N. Takata, K. Thu, and T. Miyazaki "How lubricant plays a role in the heat pump system," *EVERGREEN Joint Journal of Novel Carbon Resource Sciences & Green Asia Strategy,* **8** (1) 198–203 (2021). doi:10.5109/4372279.
33) Yanaur, Ibadurrahman, A. S. Pamitran, Gunawan, and S. Mau "Experimental investigation on the spiral pipe performance for particle-laden liquids," *EVERGREEN Joint Journal of Novel Carbon Resource Sciences & Green Asia Strategy*, **7** (4) 580–586 (2020). doi:10.5109/4150509.
34) S. S. Chauhan, and S. C. Bhaduri "Structural analysis of a four bar linkage mechanism of prosthetic knee joint using Finite Element Analysis", *EVERGREEN Joint Journal of Novel Carbon Resource Sciences & Green Asia Strategy*, 209-215 (2020). doi: 10.5109/4055220.
35) Y. Aiman, S. Syalrullail, H. Hafishah and M. N. Musa "Friction characteristic study of flat surface embedded with Micro Pit", *EVERGREEN Joint Journal of Novel Carbon Resource Sciences & Green Asia Strategy*, 304-309 (2021). doi: 10.5109/4480707.
36) T. Norfazillah, N. A. Jamaluffin, T. K. Sheng, and L. W. Kiow "Tribological study of activated carbon nanoparticle in nonedible nanofluid for machining application," *EVERGREEN Joint Journal of Novel Carbon Resource Sciences & Green Asia Strategy*, 454-460 (2021). doi: 10.5109/4480728.
37) A. C. Opia, M. K. A. Hamid, S. Samion, and C. A. N. Johnson "Nano particles additives a a promising trend in Tribology: A review on their fundamentals and mechanisms on friction and wear reduction," *EVERGREEN Joint Journal of Novel Carbon Resource Sciences & Green Asia Strategy*, 777-798 (2021). doi: 10.5109/4742121.
38) S. C. Jain, and R. Sinhasan "Performance of flexible shell journal bearings with variable viscosity lubricants", *Tribology International*, 331-339 (1983). doi: 10.1016/0301-679X(83)90043-9.
39) R. Sinhasan, and K. C. Goyal "Transient response of

a circular journal bearing lubricated with non-newtonian lubricants", *Wear*, 156(2), 385-399 (1992). doi: 10.1016/0043-1648(92)90230-6.

40) J. R. Lin "Linear stability analysis of rotor bearing system: couple stress fluid model," *Computers & Structures*, 801–809 (2001). doi: 10.1016/S0045-7949(00)00189-9
41) H. Aminkhani and M.Daliri "Effects of piezo-viscous-coupled stress lubrication squeeze film performance of parallel triangular plates," *Proc. IMechE Part J: Journal of Engineering Tribology*, 234(9) 1514–1521 (2020). doi: 10.1177/1350650119892729.
42) A. R. Reddy and S. Ismail "Tribological performance of textured parallel sliding contact under mixed lubrication condition by considering mass conservation condition and couple stress parameter," *Proc. IMechE Part J: Journal of Engineering Tribology*, 235(2) 410–422 (2021). doi: 10.1177/1350650120945080.
43) S. Akram, M Saleem, M. Y. Umair and S. Munawar "Impact of partial slip and lateral walls on peristaltic transport of a couple stress fluid in a rectangular duct," *Science Progress*, 104(2) 1–17 (2021). doi: 10.1177/00368504211013632.
44) M. Z. Mehrjardi and A. D. Rahmatabadi "Control of self-excited rotor disturbances in three-lobe journal bearing space using a couple stress fluid," *Proc. IMechE Part J: Journal of Engineering Tribology*, 236(4) 759–776 (2022). doi: 10.1177/13506501211019549.
45) K. Gangadhar, P. M. Seshakumari, M. V. S. Rao and A. J. Chamka "Biconvective transport of magnetized couple stress fluid over a radiative paraboloid of revolution," *Proc. IMechE Part J: Journal of Engineering Tribology*, 1–10 (2022). doi: 10.1177/09544089211072715.
46) S. Zhu and X. Zhang "Thermohydrodynamic lubrication analysis of misaligned journal bearing considering surface roughness and couple stress," *Proc. IMechE Part J: Journal of Engineering Tribology*, 1–18 (2022). doi: 10.1177/13506501221076893.